

Contribution from the Departments of Chemistry, Massachusetts Institute of Technology, Cambridge, Massachusetts 02139, and Colorado State University, Fort Collins, Colorado 80523

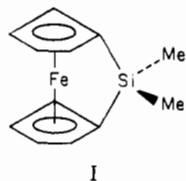
## (1,1'-Ferrocenediyl)dimethylsilane: An Electroactive Monolayer Derivatizing Reagent. Characterization of Surface-Oxygen-(Dimethylsilyl)ferrocene by Cyclic Voltammetry and Solid-State Nuclear Magnetic Resonance

ALAN B. FISCHER,<sup>1</sup> JAMES A. BRUCE,<sup>1</sup> DALE R. MCKAY,<sup>2</sup> GARY E. MACIEL,<sup>2</sup> and MARK S. WRIGHTON\*<sup>1</sup>

Received September 18, 1981

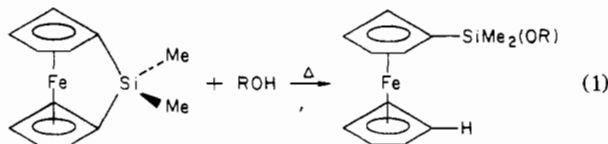
(1,1'-Ferrocenediyl)dimethylsilane (I) has been used to functionalize the surfaces of smooth Au, smooth Pt, single-crystal n-type (100) Si, (111) Si, and (111) Ge, textured (100) Si, and rough (111) Ge electrodes. For the smooth surfaces the coverage of electroactive material is between  $3.5 \times 10^{-10}$  and  $4.9 \times 10^{-10}$  mol/cm<sup>2</sup> for a large number of independent preparations. This coverage is consistent with an approximate monolayer of the ferrocene. The textured and rough surfaces give larger coverages consistent with an increase in the effective coverage by a factor of  $\sim 2$ -5. The  $E^{\circ}$  for the surface-confined ferrocene in CH<sub>3</sub>CN/0.1 M (*n*-Bu<sub>4</sub>N)ClO<sub>4</sub> on Pt or Au is +0.43 V vs. SCE. The full width of cyclic voltammetry waves at half-height on Pt and Au is  $\sim 210$  mV, consistent with nonideality in surface activities. Solid-state cross-polarization/magic-angle spinning, natural abundance, <sup>29</sup>Si, and <sup>13</sup>C NMR of high surface area silica (400 m<sup>2</sup>/g) bearing  $\sim 10^{-11}$  mol/cm<sup>2</sup> of ferrocene-centered material confirms the mode of attachment of I to be surface-O-(dimethylsilyl)ferrocene. The <sup>29</sup>Si NMR shows a single resonance due to surface-anchored material at  $\sim +7$  ppm (relative to tetramethylsilane) consistent with the -O-SiMe<sub>2</sub>Fc structure (Fc = ferrocenyl) and the <sup>13</sup>C NMR shows a singlet at  $\sim 0$  ppm (relative to tetramethylsilane) for the methyl carbons and an unresolved multiplet at  $\sim +69$  ppm (relative to tetramethylsilane) for the nonequivalent cyclopentadienyl carbons.

Characterization of surfaces bearing covalently anchored molecular reagents is essential to progress in exploiting tailored surfaces. It is also useful to have available derivatizing reagents that can themselves provide a spectroscopic handle to define certain surface characteristics. We report here a detailed cyclic voltammetry characterization of Pt, Au, Ge, and Si surfaces derivatized with (1,1'-ferrocenediyl)dimethylsilane (I). Solid-state NMR data of high surface area

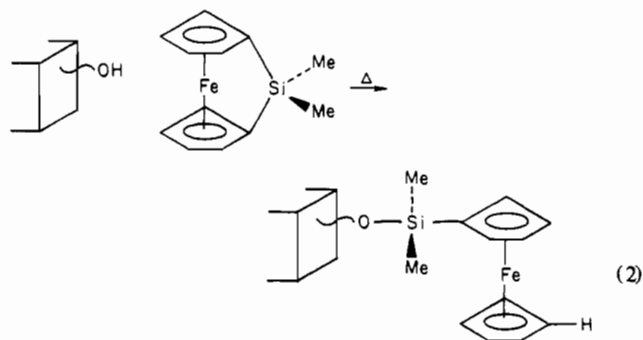


silica functionalized with I are also reported. The high surface area silica represents a sort of model for the surface of electrodes. Surface modification of electrodes by silane reagents was undertaken early by Murray and his co-workers,<sup>3</sup> and some information regarding the mode of attachment has come from X-ray photoelectron spectroscopy.<sup>3,4</sup>

The synthesis and some reaction chemistry of I have been reported previously,<sup>5</sup> and the relevant point is that it was found that ROH will effect the process represented by eq 1. It was



proposed that such a reaction with surface OH is responsible for the persistent attachment of the (dimethylsilyl)ferrocene unit to surfaces (eq 2). We have used solid-state NMR<sup>6</sup> to characterize high surface area silica functionalized with I to provide molecular specific data consistent with the structure



illustrated in eq 2. The cyclic voltammetry for smooth surfaces of Pt, Au, Ge, and Si accords well with a coverage of electroactive surface-O-(dimethylsilyl)ferrocene of less than or equal to one monolayer. Rough surfaces give larger absolute coverages of electroactive material per unit of projected area, consistent with expectation. Reagent I has the following useful set of properties: (i) reaction with -OH is fast and does not involve the release of acid as do the silyl halide reagents; (ii) the (dimethylsilyl)ferrocene is durable in two oxidation levels; (iii) the ferrocene derivatives are known to have fast heterogeneous and homogeneous electron-transfer kinetics.

### Experimental Section

**Materials.** (1,1'-Ferrocenediyl)dimethylsilane (I) was that prepared and characterized previously.<sup>5</sup> High surface area SiO<sub>2</sub> (400 m<sup>2</sup>/g) was obtained from Alfa and was functionalized with I according to the procedure outlined earlier.<sup>5</sup> Solvents used for electrochemistry were CH<sub>3</sub>CN (distilled from P<sub>2</sub>O<sub>5</sub> under Ar) or fresh absolute EtOH. The electrolyte used was polarographic grade (*n*-Bu<sub>4</sub>N)ClO<sub>4</sub> dried for 24 h under vacuum at 80 °C. Electrodes were fabricated from smooth Au or Pt foil (0.002 in. thick)<sup>7</sup> or from single-crystal n-type Si<sup>8</sup> or n-type Ge.<sup>9</sup> The polished P-doped n-type Si obtained from Monsanto was either (100) face exposed or (111) face exposed and was 0.35 mm thick with resistivities between 3 and 7 Ω cm. The

- (1) Massachusetts Institute of Technology.
- (2) Colorado State University.
- (3) Finklea, H. O.; Abruna, H.; Murray, R. W. *Adv. Chem. Ser.* **1980**, No. 184, 253 and references therein.
- (4) Allred, A. L.; Bradley, C.; Newman, T. H. *J. Am. Chem. Soc.* **1978**, *100*, 5081.
- (5) Fischer, A. B.; Kinney, J. B.; Staley, R. H.; Wrighton, M. S. *J. Am. Chem. Soc.* **1979**, *101*, 6501.
- (6) (a) Pines, A.; Gibby, M. G.; Waugh, J. S. *J. Chem. Phys.* **1973**, *59*, 569. (b) Schaefer, J.; Stejskal, E. O. *Top. Carbon-13 NMR Spectrosc.* **1979**, *3*, 283.

- (7) Wrighton, M. S.; Palazzotto, M. C.; Bocarsly, A. B.; Bolts, J. M.; Fischer, A. B.; Nadjó, L. *J. Am. Chem. Soc.* **1978**, *100*, 7264.
- (8) (a) Wrighton, M. S.; Austin, R. G.; Bocarsly, A. B.; Bolts, J. M.; Haas, O.; Legg, K. D.; Nadjó, L.; Palazzotto, M. C. *J. Am. Chem. Soc.* **1978**, *100*, 1602. (b) Bocarsly, A. B.; Walton, E. G.; Bradley, M. G.; Wrighton, M. S. *J. Electroanal. Chem. Interfacial Electrochem.* **1979**, *100*, 283. (c) Bolts, J. M.; Bocarsly, A. B.; Palazzotto, M. C.; Walton, E. G.; Lewis, N. S.; Wrighton, M. S. *J. Am. Chem. Soc.* **1979**, *101*, 1378. (d) Bruce, J. A.; Wrighton, M. S. *J. Electroanal. Chem. Interfacial Electrochem.* **1981**, *122*, 93. (e) Bocarsly, A. B.; Walton, E. G.; Wrighton, M. S. *J. Am. Chem. Soc.* **1980**, *102*, 3390.
- (9) Bolts, J. M.; Wrighton, M. S. *J. Am. Chem. Soc.* **1978**, *100*, 5257.

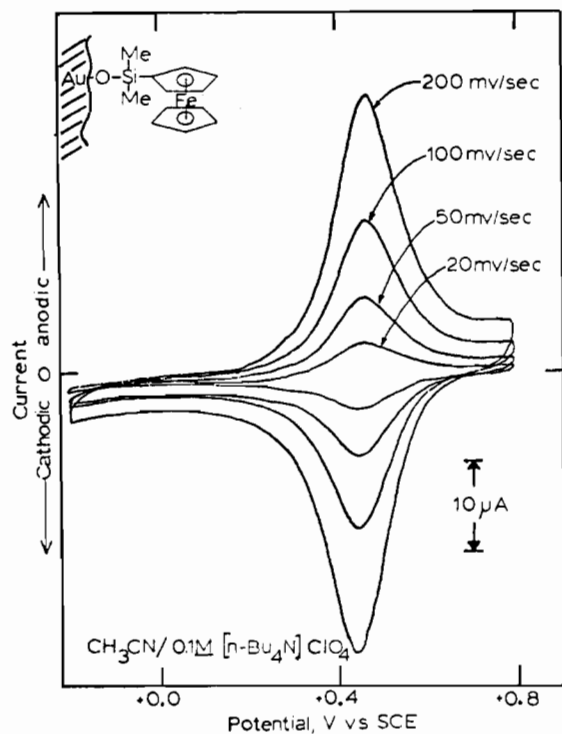


**Figure 1.** Cyclic voltammetry for Au derivatized with I. Integration of the waves shows coverage to be  $3.8 \times 10^{-10}$  mol/cm<sup>2</sup> for this 0.17-cm<sup>2</sup> electrode.

textured (100) n-type Si was prepared as described previously.<sup>8d</sup> The Sb-doped n-type Ge single crystals ( $\sim 10^{-2}$  Ω cm) were 0.5 mm thick with the (111) face exposed and were obtained from Texas Materials Laboratory, Austin, TX. Surfaces of Ge were either rough (as received) or polished with 1-μm Al<sub>2</sub>O<sub>3</sub> and were examined by microscopy (cf. Figure 4).

**Electrode Fabrication and Derivatization.** Electrodes were fabricated and pretreated for derivatization according to procedures given previously for each surface.<sup>7-9</sup> Derivatization of the surfaces with I was accomplished by soaking the pretreated electrode surfaces in isooctane solutions of I for times ranging from a few minutes to several hours. The electrodes were then washed liberally with isooctane and EtOH or CH<sub>3</sub>CN.

**Electrochemistry.** Derivatized electrodes were characterized by cyclic voltammetry in a CH<sub>3</sub>CN or EtOH solution of 0.1 M (*n*-Bu<sub>4</sub>N)ClO<sub>4</sub> under Ar at 298 K. Measurements were taken with use of the standard three-electrode setup in a one-compartment cell, and all potentials were measured vs. a saturated calomel reference electrode (SCE). The counterelectrode in all cases was Pt. Cyclic voltammetry was done with a PAR Model 175 universal programmer, a PAR Model 173-179 potentiostat, and a Houston Instruments Model 2000 X-Y recorder. The n-type Si electrodes require  $\geq E_g = 1.1$  eV illumination for the observation of the cyclic voltammetry of the surface-confined species. Illumination from a He-Ne laser at 632.8 nm ( $\sim 40$  mW/cm<sup>2</sup>) was used to irradiate the n-type Si.

**Solid-State NMR.** Solid-state cross-polarization/magic-angle spinning (CP/MAS) spectra<sup>6</sup> were obtained on a modified NT-200 spectrometer with home-built CP/MAS probes. The <sup>13</sup>C CP/MAS spectra were obtained at 50.3 MHz with use of a 1-ms contact time, a 1-s repetition time, a 4-kHz spinning speed in a Kel-F bullet rotor,<sup>10</sup> and typically about 50 000 repetitions. The <sup>29</sup>Si CP/MAS spectra, obtained at 39.7 MHz, employed a 5-ms contact time, a 2-s repetition time, a 3.5-kHz spinning speed in a Delrin bullet rotor, and typically about 10 000 repetitions. The CP/MAS experiments employed the single-contact technique,<sup>6</sup> with single-level <sup>1</sup>H decoupling at fields of about 8 kHz for the <sup>13</sup>C experiments and about 6 kHz for the <sup>29</sup>Si experiments.

**Scanning Electron Microscopy.** SEM's were taken on a Cambridge Mark 2A Stereoscan, with a resolution of 20 nm. The microscope used is equipped with a Kevex energy-dispersive X-ray analyzer.

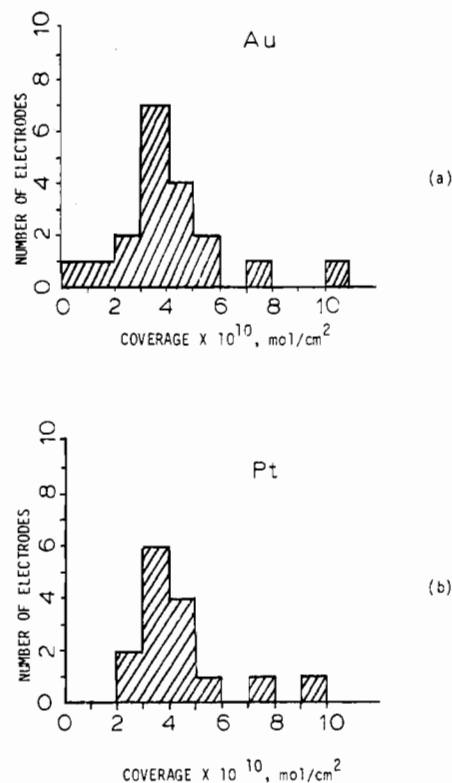


**Figure 2.** Bar graphs showing the distribution of coverages obtained for Au (a) and Pt (b) electrodes derivatized with I. A coverage value of  $3.4 \times 10^{-10}$  mol/cm<sup>2</sup> would be listed in the graph between 3.1 and 4.0, as an example. The data are from Table I.

Samples were mounted with conducting Ag paint. Generally, the samples were not gold coated since charging was not a problem at the magnifications used.

## Results and Discussion

**a. Cyclic Voltammetry of Surface-Oxygen-(Dimethylsilyl)ferrocene.** Functionalization of Pt, Au, n-Si, and n-Ge surfaces with I results in detectable electroactive material persistently attached to the surface. Figure 1 shows a typical cyclic voltammetry characterization of Au derivatized with I. Several points are noteworthy: (i) the cyclic voltammetry waves are not present for scans of a naked (nonderivatized) electrode in the same medium, consistent with the presence of a surface-confined, electroactive reagent after reaction of the pretreated surface with I; (ii) the cyclic voltammetry waves are at potentials consistent with a surface species based on ferrocene, since  $E^{0'}$  for a solution species is generally the same as for the analogous surface species; (iii) the peak-to-peak separation in the cyclic voltammetry is zero, as expected for a reversible redox couple anchored to a surface; (iv) the peak current is directly proportional to scan rate as expected for a surface-attached redox molecule. Thus, in many respects the functionalization of electrode surfaces with I accords well with expectation.<sup>11</sup>

Integration of cyclic voltammetry peaks can be used to determine the coverage of electroactive ferrocene centers on electrode surfaces functionalized with I. Coverages and other pertinent data from a large number of electrodes functionalized with I are collected in Table I. As can be seen, the Au and Pt electrodes give very similar results. Since I has only one possible point of attachment and cannot polymerize, the coverages shown should reflect monolayer, or lower, coverage. The coverages in Table I cover a very narrow range and allow an estimation of monolayer values. Figure 2 shows histograms for the number of electrodes derivatized with I that have

(10) Bartuska, V. J.; Maciel, G. E. *J. Magn. Reson.* **1981**, *42*, 312.

(11) Murray, R. W. *Acc. Chem. Res.* **1980**, *13*, 135.

Table I. Cyclic Voltammetry for Au, Pt, Ge, and Si Electrodes Functionalized with (1,1'-Ferrocenediyl)dimethylsilane<sup>a</sup>

electrode	$10^{10} \times$ coverage, <sup>b</sup> mol/cm <sup>2</sup>	anodic peak width, <sup>c</sup> mV	$E^{\circ'}$ , V (vs. SCE) <sup>d</sup>	electrode	$10^{10} \times$ coverage, <sup>b</sup> mol/cm <sup>2</sup>	anodic peak width, <sup>c</sup> mV	$E^{\circ'}$ , V (vs. SCE) <sup>d</sup>
smooth Au				n-type Si (111) (polished)			
1	7.1	180	+0.425	1	4.0	210	<i>e</i>
2	4.3	250	+0.440	2	5.4	190	<i>e</i>
3	2.5	180	+0.440	3	4.3	220	<i>e</i>
4	3.8	190	+0.425	4	3.7	140	<i>e</i>
5	4.1	300	+0.450	5	2.9	160	<i>e</i>
6	3.5	190	+0.420	6	3.8	170	<i>e</i>
7	1.1	220	+0.435	7	3.9	190	<i>e</i>
8	3.3	240	+0.445	8	5.9	190	<i>e</i>
9	2.9	260	+0.430	9	3.2	170	<i>e</i>
10	5.7	200	+0.450	10	7.2	190	<i>e</i>
11	10.2	280	+0.430	11	3.3	180	<i>e</i>
12	3.3	210	+0.405	12	4.1	230	<i>e</i>
13	4.2	170	+0.430	13	6.7	160	<i>e</i>
14	1.0	200	+0.410	average	4.4	185	<i>e</i>
15	3.8	190	+0.425	n-type Si (100) (polished)			
16	3.9	190	+0.430	1	5.4	200	<i>e</i>
17	5.0	210	+0.425	2	3.5	160	<i>e</i>
18	4.3	170	+0.440	3	4.4	220	<i>e</i>
19	3.7	190	+0.435	4	7.6	210	<i>e</i>
average	4.1	212	+0.431	5	3.6	220	<i>e</i>
smooth Pt				average	4.0	202	<i>e</i>
1	4.1	210	+0.440	n-type Si (100) (textured)			
2	3.7	190	+0.425	1	8.1	250	<i>e</i>
3	9.3	300	+0.435	2	11	270	<i>e</i>
4	2.3	220	+0.420	3	15	250	<i>e</i>
5	4.5	230	+0.425	4	11	250	<i>e</i>
6	3.6	170	+0.450	5	12	210	<i>e</i>
7	3.9	200	+0.435	6	5.9	200	<i>e</i>
8	2.4	180	+0.430	7	7.8	280	<i>e</i>
9	4.5	190	+0.420	8	14	200	<i>e</i>
10	4.5	210	+0.440	average	10.6	239	<i>e</i>
11	3.9	240	+0.445	n-type Ge (111) (polished)			
12	5.6	180	+0.430	1	3.5	100	<i>e</i>
13	7.2	200	+0.435	2	4.0	90	<i>e</i>
14	3.4	210	+0.440	n-type Ge (111) (rough)			
15	3.3	170	+0.425	1	9.2	140	<i>e</i>
average	4.7	207	+0.433	2	21	130	<i>e</i>
				3	21	160	<i>e</i>
				4	16	170	<i>e</i>
				5	23	220	<i>e</i>
				6	14	160	<i>e</i>
				7	20	180	<i>e</i>
				average (rough)	17	165	<i>e</i>

<sup>a</sup> Data are for electrodes scanned at 100 mV/s in (CH<sub>3</sub>CN or EtOH)/0.1 M (*n*-Bu<sub>4</sub>N)ClO<sub>4</sub> at 25 °C. <sup>b</sup> Coverage is from the integration of the anodic cyclic voltammetry wave. <sup>c</sup> Width of the anodic wave at half-height. <sup>d</sup> Formal potential,  $E^{\circ'}$ , of the surface species is taken to be the average position of anodic and cathodic current peaks on the reversible Pt or Au surfaces. <sup>e</sup> n-Type semiconductors do not give reversible electrochemistry (cf. text). Coverages were determined by cyclic voltammetry under illumination for n-type Si, 632.8 nm (~40 mW/cm<sup>2</sup>); the n-type Ge used gives nearly the same cyclic voltammetry with and without illumination.

certain ranges of coverage. These electrodes were derivatized for varying lengths of time and with varying concentrations of I, both Pt and Au mixed. The histograms show rough upper limits on coverage that should represent the attainment of monolayer levels. Slight variations in surface roughness or the number of surface -OH groups created by pretreatment would explain the lack of an extremely sharp cutoff in coverage.

A coverage value of  $4 \times 10^{-10}$  mol/cm<sup>2</sup> is a rough cutoff point for both the Au and the Pt data in the histograms. If the fact that mirror-polished surfaces have a roughness factor of 1.2–1.8 is taken into account, the actual area per molecule would be in the range 50–76 Å<sup>2</sup>/molecule. Both Pt and Au single crystals have fcc lattices with  $a = 4 \text{ \AA}$ <sup>12</sup> so there are approximately 12.5 atoms/100 Å<sup>2</sup> for the metal electrodes used here. The limiting coverage value of  $4 \times 10^{-10}$  mol/cm<sup>2</sup> re-

quires that only 19% of the surface metal atoms be involved in M–O–Si bonding. Monosubstituted ferrocenes, e.g., (diethylsilyl)ferrocene, have a density of ~1.0–1.3 g/cm<sup>3</sup>.<sup>13</sup> From this range of densities we would expect each surface–O–(dimethylsilyl)ferrocene to occupy ~55 Å<sup>2</sup> of surface area, assuming the molecular entity occupies a cube. This means that the density predicts a close-packed monolayer to be associated with a coverage of  $\sim 3 \times 10^{-10}$  mol/cm<sup>2</sup>, in good agreement with values found for smooth electrode surfaces.

Cyclic voltammetric waves for Au and Pt electrodes derivatized with I are slightly narrower than for electrodes derivatized with (1,1'-ferrocenediyl)dichlorosilane (II), which usually gives polymeric coverages of ferrocene-centered redox material.<sup>7</sup> If the width of the cyclic voltammetric waves for

(12) Kittel, C. "Introduction to Solid State Physics"; Wiley: New York, 1956; p 40.

(13) (a) Nanetkin, N. S.; Chernysheva, T. I.; Babare, L. V. *Zh. Obshch. Khim.* **1964**, *34*, 2258. (b) Von Gerd, G.; Hallensleben, M. L. *Makromol. Chem.* **1967**, *104*, 77. (c) Paton, W. F.; Corey, E. R.; Corey, J. Y.; Glick, M. D.; Mislow, K. *Acta Crystallogr., Sect. B* **1977**, *B33*, 268.

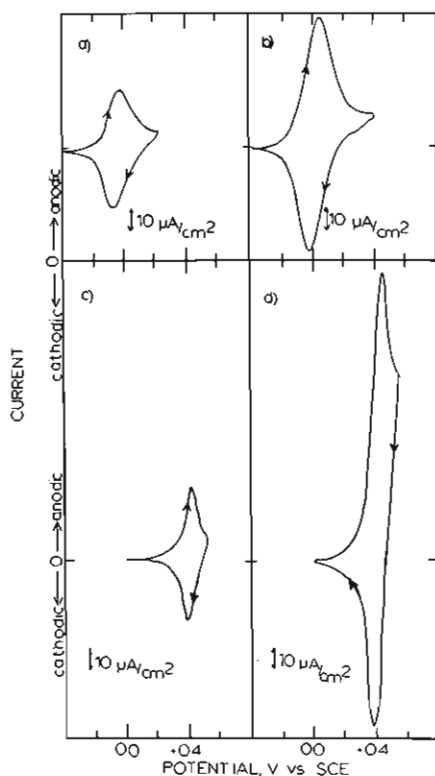


**Figure 3.** Representative cyclic voltammograms for n-type Si and Ge functionalized with I. The data are for representative samples of polished (100) Si (a), textured (100) Si (b), polished (111) Ge (c), and rough (111) Ge (d). Data for Ge are from surfaces represented by Figure 4. Illumination for the n-type Si was from a He-Ne laser at 632.8 nm ( $\sim 40$  mW/cm<sup>2</sup>).

the multilayer electrodes made with II were due to interactions within the multilayer structure, then one would expect to see substantially sharper waves for the submonolayer and monolayer coverages obtained by derivatization with I. The average value of the peak widths from Table I is only 25 mV smaller than the value of 236 mV obtained for Au electrodes derivatized with II.<sup>7</sup> This difference is small compared to the differences in coverage being compared and the fact that the value expected theoretically is 90 mV.<sup>11</sup> This small difference is also consistent with the lack of correlation found between the peak widths and coverage for electrodes derivatized with II. The conclusion is that the width of the cyclic voltammetry peaks for the ferrocene-centered derivatizing reagents is independent of whether oligomers are present. The  $>90$  mV width of the cyclic voltammetry waves is attributable to nonideality of surface activity.<sup>11</sup>

Representative cyclic voltammograms for n-type Si and Ge are given in Figure 3. Peak widths of the cyclic voltammetry waves for n-type Si and Ge electrode surfaces derivatized with I are generally in the same range as for Pt and Au, but interestingly there are occasionally narrow waves ( $\sim 90$  mV width at half-height). Reproducibility of coverage is quite good for polished surfaces. The coverages are quite similar to those for Au and Pt, and the coverage of n-type Si is independent of whether the (100) or (111) face is functionalized.

The major variation in surface coverage from derivatization of n-type Si with I comes from the functionalization of "textured" (100) n-type Si. Textured (100) n-type Si is an etched surface<sup>8d,14</sup> that reveals (111) planes, and a perfect etch increases actual surface area by a factor of  $<4$  from geometrical considerations. As shown in Table I the surface of

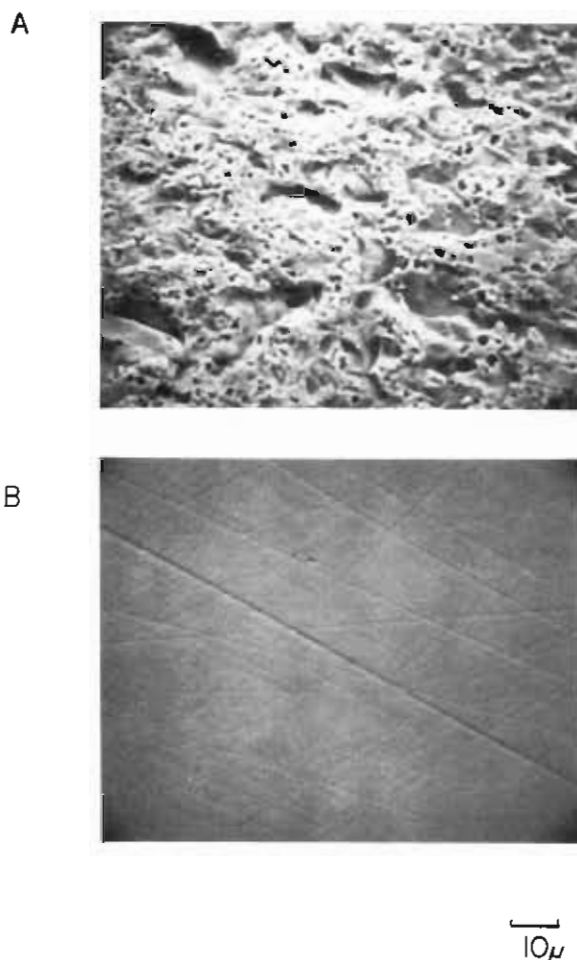


**Figure 4.** Scanning electron micrographs of representative samples of rough (A) and polished (B) (111) Ge used in the derivatization with I. Coverage data are given in Table I for such surfaces.

textured (100) n-type Si gives approximately a factor of 2 increase in the amount of electroactive material per unit of projected area.

Functionalization of polished vs. roughened (111) n-type Ge surfaces with I (Figure 4) also reveals substantial differences in the amount of electroactive material per unit of projected area. As the data in Table I show, the roughened surfaces like that in Figure 4A bind up to a factor of  $\sim 5$  more electroactive material per unit of projected area.

The main conclusion that we draw from functionalization of polished vs. textured and roughened surfaces is that functionalization with reagent I appears to give the proper qualitative result, namely, an increase in the amount of bound material per unit of projected surface area when the actual surface area is increased. Increasing the number of electroactive centers per unit of projected area is an important objective when the derivatization is carried out in order to effect catalysis of some desirable redox process. For example, the photoelectrochemical oxidation of  $I^-$  to  $I_3^-$  has been observed to occur at n-type Si functionalized with I.<sup>8c</sup> The observed photocurrent is directly proportional to surface coverage of ferrocene centers.<sup>15</sup> Thus, derivatization of roughened Ge or textured Si can give improved performance compared to that of the polished surfaces.

While the coverages and cyclic voltammetry peak widths of electroactive material from I on smooth n-type Ge and Si are similar to the same parameters on Au and Pt (Table I),

(14) (a) Kern, W. *RCA Rev.* **1978**, *39*, 287. (b) Baraona, C.; Brandhorst, H. *Conf. Rec. IEEE Photovoltaic Spec. Conf.* **1975**, *11*, 44. (c) Restrepo, F.; Backus, C. E. *IEEE Trans. Electron Devices* **1976**, *23*, 1195.

(15) (a) Lewis, N. S.; Bocarsly, A. B.; Wrighton, M. S. *J. Phys. Chem.* **1980**, *84*, 2033. (b) Lewis, N. S.; Wrighton, M. S. *ACS Symp. Ser.* **1981**, *No. 146*, 37.

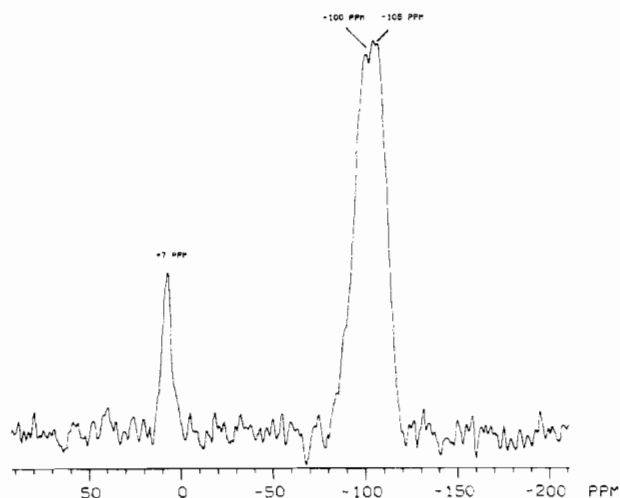


**Figure 5.** CP/MAS solid-state  $^{29}\text{Si}$  NMR of high surface area  $\text{SiO}_2$  functionalized with I.

the position of the peaks on these n-type semiconductors depends on the intensity of  $\geq E_g$  illumination. The n-type Ge has an  $E_g = 0.7$  eV, and photoeffects are quite small.<sup>9</sup> Oxidation of the surface-confined ferrocene can occur on the n-type Ge in the dark, near the same position as on Au and Pt, provided low scan rates ( $<100$  mV/s) are used. Upon illumination with  $\geq E_g$  light the oxidation can be observed to occur up to 200 mV more negative than that at Pt or Au, consistent with data from derivatization with II. The  $\sim 200$ -mV negative shift is a measure of the extent to which the ferrocene oxidation can be driven uphill with light.

In contrast to the n-type Ge, the n-type Si has a larger  $E_g$ , 1.1 eV, and dark oxidation of the surface ferrocene does not occur at potentials as positive as +0.8 V vs. SCE. Illumination with  $\geq E_g$  light effects the oxidation of the surface-bound ferrocene center at potentials as negative as  $\sim -0.1$  V vs. SCE. This represents a negative shift of  $\sim 500$  mV relative to the oxidation peak position on Pt or Au.<sup>8</sup>

With the assumption that the actual redox energetics for the surface-O-(dimethylsilyl)ferrocene are unaffected by the surface,<sup>11</sup> the interpretation of the  $\sim 200$ -mV and  $\sim 500$ -mV negative shift of the oxidation peak on illuminated n-type Ge and n-type Si, respectively, is that the surface redox reagent actually attains its  $E^{o'}$  at an electrode potential that is more negative. That is, the ratio of ferrocenium/ferrocene on the surface becomes unity at an electrode potential under illumination where only ferrocene would be present in the dark. The ability to drive the oxidation process in this uphill sense is the basis of photoelectrochemical energy conversion devices based on n-type semiconductors. The oxidizing power of the photogenerated surface oxidant is used to effect oxidation processes of solution species.

**b. Solid-State NMR of High Surface Area Silica Derivatized with I.** Cyclic voltammetry data accord well with the conclusion that I functionalizes electrode surfaces via eq 2. However, such data do not provide molecular specific information. Recent success with cross-polarization/magic-angle spinning (CP/MAS) solid-state NMR in characterizing silica surfaces<sup>16</sup> prompted us to use this technique to characterize high surface area  $\text{SiO}_2$  (400  $\text{m}^2/\text{g}$ ) after functionalization with I. High surface area  $\text{SiO}_2$  allows the preparation of surface-confined material that obviously involves a large amount of the molecular entity per unit mass. The sample of  $\text{SiO}_2$

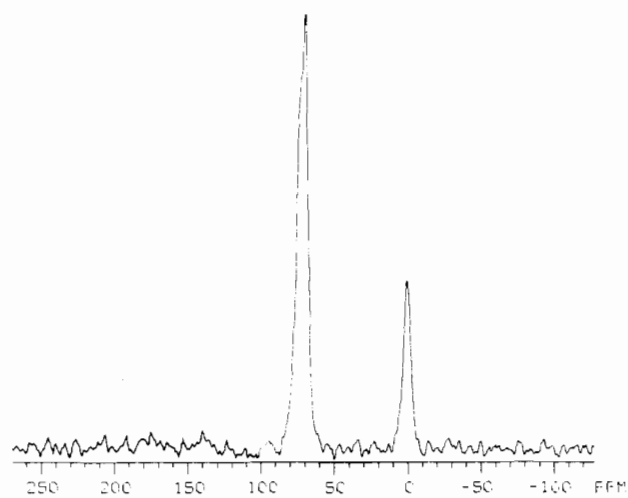


**Figure 6.** CP/MAS solid-state  $^{13}\text{C}$  NMR of high surface area  $\text{SiO}_2$  functionalized with I.

derivatized with I was prepared in a manner identical with that prepared and characterized by UV-vis photoacoustic spectroscopy earlier.<sup>5</sup> The photoacoustic spectroscopy of the derivatized  $\text{SiO}_2$  is consistent with a ring-opening reaction as in eq 2 to anchor the (dimethylsilyl)ferrocene unit.

The  $^{13}\text{C}$  and  $^{29}\text{Si}$  CP/MAS spectra are of quality (resolution and intensity) that is similar to what has been observed for derivatized silica systems.<sup>16</sup> The  $^{29}\text{Si}$  spectrum shows a peak at 7 ppm that can be assigned to the  $-\text{Si}(\text{CH}_3)_2-$  moiety and a broad band centered around  $-102$  ppm (Figure 5). The latter band is assigned to silicon atoms at the surface of the silica gel, for which shifts of  $-91$ ,  $-100$ , and  $-109$  ppm have been assigned previously<sup>5</sup> to silicon moieties of the types  $(\text{HO})_2\text{Si}^*(\text{OSi}-)_2$ ,  $\text{HOSi}^*(\text{OSi}-)_3$ , and  $\text{Si}^*(\text{OSi}-)_4$ , respectively. In the  $^{13}\text{C}$  CP/MAS spectrum, Figure 6, the peak near 0 ppm can be assigned to the methyl groups. The unsymmetrical  $^{13}\text{C}$  resonance that peaks at about 69 ppm is assignable to resonances of the cyclopentadienyl group. The shoulder on the low-shielding side of that peak can be "resolved" by resolution enhancement, but not in a manner that would lead to a convincing interpretation of specific nonequivalent carbons.

The  $^{29}\text{Si}$  CP/MAS spectrum of nonderivatized  $\text{SiO}_2$  used in this study does exhibit resonances in the  $-90$  to  $-110$  ppm region consistent with the presence of the various  $\text{SiOH}$  functionalities mentioned above. The  $-90$  to  $-110$  ppm region is affected by derivatization with I in a manner consistent with consumption of some, but not all, surface  $\text{SiOH}$  groups. Analysis<sup>5</sup> of the  $\text{SiO}_2$  derivatized with I shows that the coverage of surface-O-(dimethylsilyl)ferrocene is  $\sim 10^{-11}$  mol/ $\text{cm}^2$  or more than a factor of 10 lower than on the polished electrode surfaces (Table I). Thus, the coverage is consistent with the NMR detection of remaining surface  $\text{SiOH}$  functionality. The position of the  $^{29}\text{Si}$  resonance for the (dimethylsilyl)ferrocene accords well with the position of the  $^{29}\text{Si}$  resonance for chlorodimethylsilyl groups on  $\text{SiO}_2$  surfaces.<sup>16</sup> The single peak confirms the existence of only one type of dimethylsilyl group from functionalization with I. In particular, cleavage of both Si-C bonds of I is ruled out, since resonances for various methylsilyl and dimethylsilyl species are well resolved from that which we actually observe.<sup>16a</sup> Thus, the solid-state CP/MAS spectra of  $\text{SiO}_2$  derivatized with I fully confirm the representation in eq 2.

The high surface area  $\text{SiO}_2$  is an excellent model for the surfaces of Si, since the Si invariably has a thin air oxide<sup>17</sup>

(16) (a) Sindorf, D. W.; Maciel, G. E. *J. Am. Chem. Soc.* **1981**, *103*, 4263. (b) Maciel, G. E.; Sindorf, D. W.; Bartuska, V. J. *J. Chromatogr.* **1981**, *205*, 438. (c) Maciel, G. E.; Sindorf, D. *J. Am. Chem. Soc.* **1980**, *102*, 7606.

(17) (a) Schmidt, P. F.; Michel, W. *J. Electrochem. Soc.* **1957**, *104*, 230. (b) Raider, S. I.; Flitsch, R.; Palmer, M. J. *Ibid.* **1975**, *122*, 413.

that should provide the sort of SiOH surface functionality present on the SiO<sub>2</sub>. We conclude that attachment of I to n-type Si proceeds as on high surface area SiO<sub>2</sub>. Models of the oxide/hydroxides of Pt, Au, and Ge have not been studied by solid-state NMR, but we believe that the electrochemical data are consistent with a mode of reaction as illustrated in eq 2. The reason for the relatively low coverage of I on high surface area SiO<sub>2</sub> vs. the smooth surface is not clear. It is possible that not all surface SiOH's are accessible to the derivatization agent.

**Acknowledgment.** Work at MIT was supported by the United States Department of Energy, Office of Basic Energy Sciences, Division of Chemical Sciences. This work was aided by the Colorado State University Regional NMR Center, funded by National Science Foundation Grant No. CHE78-18581. D.R.M. and G.E.M. also gratefully acknowledge the assistance of Dr. Bruce L. Hawkins.

**Registry No.** I, 72380-68-8; Au, 7440-57-5; Pt, 7440-06-4; Ge, 7440-56-4; Si, 7440-21-3; SiO<sub>2</sub>, 7631-86-9.

Contribution from the Institute of Inorganic Chemistry, University of Fribourg, P erolles, CH-1700 Fribourg, Switzerland

## Formation of Ternary Copper(II) Complexes at the Surface of Silica Gel As Studied by ESR Spectroscopy

ALEX VON ZELEWSKY\* and JEAN-MARIE BEMTGEN

Received July 30, 1981

ESR spectroscopy is applied in the investigation of the adsorption behavior of Cu(II) complexes and Cu(II) ions on silica gel. With this method, results of pH titration measurements,<sup>1,2</sup> which indicate the formation of ternary surface complexes involving some ligands and chelating SiO<sup>-</sup> groups, are confirmed. N-chelating ligands with conjugated  $\pi$  systems enhance the adsorption by formation of ternary surface complexes (bpy, phen, terpy), whereas aliphatic amine ligands (en) attenuate adsorption, as compared to Cu<sup>2+</sup> ions. Unsaturated ligands having N/O mixed chelates (pic) form less stable ternary surface complexes, as compared to N chelates. Saturated ligands (gly) show, again, attenuation of adsorption. Fully coordinated cationic complexes are adsorbed on the negatively charged surface of silica gel at pH values above ca. 5.5 by Coulombic forces. Neutral or anionic complexes are not at all adsorbed at high pH values. Some complexes (Cu(bpy)<sub>2</sub><sup>2+</sup>, Cu(phen)<sub>2</sub><sup>2+</sup>, and Cu(pic)<sub>2</sub>) adsorb even in quite acidic solution (pH range of 1-4). This is interpreted as being due to the formation of ternary chelates with surface SiOH groups.

### Introduction

The investigation of adsorption equilibria between oxide surfaces and solutes in liquid solutions is a subject of interest in various fields of chemistry. In particular, equilibria involving transition-metal complexes have been studied in recent years in regard to natural water systems. The work of Stumm et al.<sup>3-6</sup> and Schindler et al.<sup>1,7-11</sup> has shown that a description of the adsorption of metal ions on oxide surfaces has to take into account the complex formation between the ions and the ionized surface. The coordinate binding model<sup>7-9,12</sup> gives an adequate description of the adsorption phenomena. A striking manifestation of surface complex formation has been found by Schindler et al.<sup>1</sup> They found a strongly enhanced or diminished adsorption for Cu(II) depending on ligands bound to Cu<sup>2+</sup> in solution. The enhancement of, e.g., the adsorption of Cu(bpy)<sub>2</sub><sup>2+</sup>, as compared to the aquated Cu<sup>2+</sup> ion, is analogous to the stabilization of ternary complexes in solution.<sup>13,14</sup>

Hitherto, the metal complex adsorption equilibria were investigated by titration methods.<sup>1</sup> No direct structural information is available from these measurements.

In the present paper, ESR spectroscopy is applied as a tool in determining adsorption equilibria, which can yield structural information on adsorbed species. In principle, ESR spectroscopy can also easily distinguish between freely tumbling complexes in solution and immobilized adsorbed species. In fluid solution with a rotational correlation time of the order of  $\tau_c = 10^{-10}$  s, the anisotropic contributions to the *g* and hyperfine coupling constants are virtually averaged. In the adsorbed state, the anisotropic interactions contribute fully to the spectra. The line shapes expected are the same as in other immobilized nonoriented systems such as, e.g., polycrystalline samples and frozen solutions. These line shapes are well understood,<sup>15</sup> and the spectra can be accordingly analyzed.

This ESR method can be applied to adsorption processes in all such cases where a transition-metal ion yields resolved spectra at temperatures at which the liquid phase is in a fluid state. Only then can the distinction between mobile and immobilized species be made. Cu<sup>2+</sup> as a d<sup>9</sup>, *S* = 1/2 system fulfills this requirement as it yields resolved ESR spectra at room temperature and even above. Since this ion has been investigated by titration methods in the past, a comparison between results obtained in completely independent ways is possible.

### Experimental Section

**Reagents.** The following aqueous solutions (in twice distilled water) with a constant ionic strength (NaNO<sub>3</sub> = 0.1 M) and a defined metal:ligand ratio were prepared (if not otherwise indicated, the total

- (1) A. C. M. Bourg, S. Joss, and P. W. Schindler, *Chimia*, **33**, 19 (1979).
- (2) A. C. M. Bourg, and P. W. Schindler, *Inorg. Nucl. Chem. Lett.*, **15**, 225 (1979).
- (3) C. P. Huang and W. Stumm, *J. Colloid Interface Sci.*, **43**, 409 (1973).
- (4) H. Hohl and W. Stumm, *J. Colloid Interface Sci.*, **55**, 281 (1976).
- (5) R. Kummert and W. Stumm, *J. Colloid Interface Sci.*, **75**, 373 (1980).
- (6) W. Stumm, R. Kummert, and L. Sigg, *Croat. Chem. Acta*, **53**, 291 (1980).
- (7) P. W. Schindler and H. R. Kamber, *Helv. Chim. Acta*, **51**, 1781 (1968).
- (8) P. W. Schindler, E. W alti, and B. F urst, *Chimia*, **30**, 107 (1976).
- (9) P. W. Schindler, B. F urst, R. Dick, and P. U. Wolf, *J. Colloid Interface Sci.*, **55**, 469 (1976).
- (10) A. C. M. Bourg and P. W. Schindler, *Chimia*, **32**, 166 (1978).
- (11) A. C. M. Bourg, *Manage. Control Heavy Met. Environ., Int. Conf.*, 446 (1979).
- (12) B. F urst, Ph.D. Thesis, University of Berne, 1976.
- (13) H. Sigel, *Angew. Chem.*, **11**, 391 (1975).
- (14) H. Sigel, *Inorg. Chim. Acta*, **6**, 195 (1972).

- (15) J. E. Wertz and J. R. Bolton, "Electron Spin Resonance, Elementary Theory and Practical Applications", McGraw-Hill, New York, 1972.